Superconductivity under a ferromagnetic molecular field

Kazushige Machida
Department of Physics, Kyoto University, Kyoto 606, Japan

Hiizu Nakanishi
Department of Physics, Faculty of Science and Technology, Keio University, Yokohama 223, Japan
(Received 2 January 1984)

Superconductivity under a ferromagnetic molecular field is investigated theoretically based on a one-dimensional electron-band model. By using an exact solution which takes into account infinite numbers of higher harmonics for the Bogoliubov—de Gennes equation, it is demonstrated that the spatially modulated superconducting state with a distorted sinusoidal wave is stabilized in the high-field region. A key feature of the solution is a soliton lattice structure which has a two-energy-gap structure and is accompanied by a spin-density polarization of the conduction electrons. The coexistence phase observed in $ErRh_4B_4$, which consists of ferromagnetism, superconductivity, and a sinusoidally modulated magnetic state, is successfully interpreted in terms of this modulated superconducting state.

I. INTRODUCTION

There has been much attention focused on the problem of the interplay between magnetism and superconductivity. The antiferromagnetism carried by the $4f$ localized moments is found to coexist with superconductivity in rare-earth ternary compounds such as $SmRh_4B_4$ and RMo_6S_8 (R is Gd, Tb or Dy). We understand quite thoroughly this coexistence phenomenon theoretically.[1] On the other hand, there is much controversy about the possibility of the coexistence of ferromagnetism and superconductivity.

Recently, a remarkable neutron experiment has been done by Sinha *et al.*[2] using single crystalline samples of the ferromagnetic superconductor $ErRh_4B_4$ (ERB) which will underlie the future theoretical development of this field. Their results and experimental data accumulated so far[1-4] are summarized as follows. Upon decreasing the temperature from the upper superconducting transition temperature $T_{c1}\simeq 8.7$ K ferromagnetism appears at $T=T_M\simeq 1.2$ K, accompanied by a sharp lambda-type peak in the specific heat.[3] The sinusoidally modulated phase also sets in at almost the same temperature, which is evidenced by the appearance of satellite peaks associated with the main ferromagnetic peaks. This sinusoidally modulated phase is characterized by a wavelength $\simeq 100$ Å, which is almost temperature independent. With further decrease of temperature, the system reenters the normal state at T_{c2} ($\simeq 0.7$ K, cooling; and 0.76 K, warming), showing hysteretic behavior. The ferromagnetism persists down to $T=0$ while the sinusoidally modulated phase abruptly disappears at T_{c2}. Similar successive phase transitions are also observed in another ferromagnetic superconductor $HoMo_6S_8$ (HMS).[4] It is important to note that at $T=T_{c2}$ the magnetization of the ferromagnetic component reaches ~ 70—$80\,\%$ of the saturation value of the $4f$ localized moment. This fact is also observed in the previous neutron experiment[2] using polycrystalline samples of ERB.

It is impossible to conclude solely by neutron experiments whether or not the two scatterings of the satellite and ferromagnetic components come from the same place in the sample. This experimental ambiguity causes much controversy among theorists. Almost all existing theories[5-9] on ferromagnetic superconductors lead to a spatially modulated magnetic phase supplemented by a domain structure of ferromagnetism, assuming that the two scatterings come from different places and denying the coexistence of ferromagnetism and superconductivity. In view of the facts that the widths of the satellite and ferromagnetic peaks are resolutionally limited, exhibiting a true long-range order with the magnetic correlation length[2] extended over 10000 Å and that a sharp lambda-type anomaly in the specific heat at T_M is observed, we take an alternative view of accepting that the three orderings of the superconductivity, sinusoidally modulated phase, and ferromagnetism really coexist within the same place in a system. We pursue this possibility further[10,11] in this paper.

Suppose that the coexistence of ferromagnetism and superconductivity is achieved in ERB, then the ferromagnetic molecular field ($\sim$order of a few hundred kG) exerted by the $4f$ localized moments through the so-called sf exchange interaction between the conduction electrons and localized $4f$ electrons becomes essential. We can safely neglect the dipolar field ($\sim$a few kG) coming from the electromagnetic interaction. In fact, the antiferromagnetic molecular-field effect[12] of the sf exchange interaction explains the essential features of the experimental data on several antiferromagnetic superconductors.

Fulde and Ferrell[13] and Larkin and Ovchinnikov[14] independently studied the problem of superconductivity under a uniform field which acts on the electron spin. They conclude that a spatially nonuniform superconduct-

ing state is stabilized in a certain field region. In particular, Larkin and Ovchinnikov claim that among various solutions the sinusoidally modulated phase of the order parameter is most stable near its transition temperature by using a three-dimensional Fermi-surface model. Takada and Izuyama[15] give a detailed calculation for the helical solution investigated by Fulde and Ferrell.

The purposes of the present paper are twofold: By confining ourselves to a one-dimensional electron-band model and utilizing the mathematical equivalence[16] of the present problem to the one-dimensional Peierls-Fröhlich system, where an exact solution was found,[17–19] we will give an exact solution of the problem within the mean-field approximation which takes into account infinite orders of higher harmonics. We will investigate detailed physical properties of the sinusoidal solution which will be proved to be more stable than the helical solution down to $T=0$. The other purpose is to examine the experimental data on ERB, especially the recent neutron work in the context of the present complete solution. We have already given a rough analysis of the experimental data on ERB and HMS in previous papers[10,11] in terms of the same idea of the spatially modulated superconductivity state.

The arrangement of this paper is as follows. In the next section we formulate the stability problem of the superconducting state under a ferromagnetic molecular field in a one-dimensional electron-band model and demonstrate that the derived Bogoliubov–de Gennes (BdG) equation[20] is the same as that of the one-dimensional Peierls system where several authors[17–19] have obtained the exact solutions. We briefly summarize their results in Sec. III in order to set up the basic self-consistent equations that will be used later. The various physical properties of the solution are investigated in Sec. IV, including the phase diagram, energy-gap structure, and superconducting order parameter. We calculate the conduction-electron spin polarization associated with the solution in Sec. V. An interpretation of the experimental data on ERB is given in Sec. VI. The final section is devoted to a summary and discussion.

II. FORMULATION

We start with the following sf exchange Hamiltonian which describes the interaction between the localized $4f$ moment system of rare-earth ions embedded in periodic lattice sites and the conduction electrons:

$$\mathcal{H}=\mathcal{H}_s+\mathcal{H}_{sf} ,$$
$$\mathcal{H}_s=\int d^3x \left[\sum_\sigma \psi_\sigma^\dagger(x)\epsilon(\vec{\nabla})\psi_\sigma(x) - \frac{g}{2}\sum_{\sigma,\sigma'}\psi_\sigma^\dagger(x)\psi_{\sigma'}^\dagger(x)\psi_{\sigma'}(x)\psi_\sigma(x)\right] , \tag{2.1}$$
$$\mathcal{H}_{sf}=-\tfrac{1}{2}I(g_J-1)\sum_{i,\mu,\nu}\vec{\mathrm{J}}_i\cdot\vec{\sigma}_{\mu\nu}\psi_\mu^\dagger(R_i)\psi_\nu(R_i)$$
$$=-\tfrac{1}{2}I(g_J-1)\sum_{i,\mu,\nu}\int d^3x\,\vec{\mathrm{J}}(R_i-x)\cdot\vec{\sigma}_{\mu\nu}\psi_\mu^\dagger(x)\psi_\nu(x) ,$$

where g is the attractive electron-electron interaction, I is the exchange constant, g_J is the Landé factor, and $\vec{\mathrm{J}}$ is the total angular momentum of a rare-earth ion. Applying the molecular-field approximation to the sf Hamiltonian, we obtain

$$\mathcal{H}_{sf}=-\sum_\sigma\int d^3x\, h\sigma\psi_\sigma^\dagger(x)\psi_\sigma(x) ,$$
$$h=\tfrac{1}{2}I(g_J-1)\sum_i\langle\vec{\mathrm{J}}_z(R_i-x)\rangle \tag{2.2}$$

which acts to shift the Fermi energies of the spin-up and -down electron bands, inducing Zeeman splitting. Note that h has the dimension of energy. We have neglected the spatial variation of the molecular field. The problem reduces to examining the stability of the superconducting state under a uniform field h.

Now we confine our discussion to the one-dimensional band model with linear dispersion. We introduce two kinds of electron fields: a left-moving electron field $\phi_\sigma(x)$ and a right-moving electron field $\psi_\sigma(x)$. We can rewrite the above Hamiltonian as follows:

$$\mathcal{H}=\mathcal{H}_0+\mathcal{H}_{\mathrm{ex}}+\mathcal{H}_{\mathrm{int}} ,$$
$$\mathcal{H}_0=\sum_\sigma\int dx[\psi_\sigma^\dagger(x)v_F(p-p_F)\psi_\sigma(x) + \phi_\sigma^\dagger(x)v_F(-p-p_F)\phi_\sigma(x)] , \tag{2.3}$$
$$\mathcal{H}_{\mathrm{ex}}=h\sum_{\sigma,\tau}\int dx[\psi_\sigma^\dagger(x)(\sigma_3)_{\sigma\tau}\psi_\tau(x) + \phi_\sigma^\dagger(x)(\sigma_3)_{\sigma\tau}\phi_\tau(x)] ,$$

where v_F and p_F are the Fermi velocity and momentum. In terms of the order parameters defined by

$$\Delta_{\mathrm{I}}(x)=g\langle\psi_\uparrow(x)\phi_\downarrow(x)\rangle,\quad \Delta_{\mathrm{I}}^*(x)=g\langle\phi_\downarrow^\dagger(x)\psi_\uparrow^\dagger(x)\rangle ,$$
$$\Delta_{\mathrm{II}}(x)=g\langle\phi_\uparrow(x)\psi_\downarrow(x)\rangle,\quad \Delta_{\mathrm{II}}^*(x)=g\langle\psi_\downarrow^\dagger(x)\phi_\uparrow^\dagger(x)\rangle , \tag{2.4}$$

the interaction Hamiltonian within the mean-field approximation can be rewritten as

$$\mathcal{H}_{\mathrm{int}}=-\int dx\{\Delta^*(x)[\psi_\uparrow(x)\phi_\downarrow(x) + \phi_\uparrow(x)\psi_\downarrow(x)]+\mathrm{H.c.}\} , \tag{2.5}$$

where

$$\Delta(x)=\Delta_{\mathrm{I}}(x)+\Delta_{\mathrm{II}}(x)=\Delta_r(x)+i\Delta_i(x) .$$

Here we introduce the Nambu notation

$$\Psi^\dagger(x)=(\psi_\uparrow^\dagger(x),\phi_\downarrow(x)),\quad \Phi^\dagger(x)=(\phi_\uparrow^\dagger(x),\psi_\downarrow(x))$$

and arrive at

$$\mathcal{H}=\int dx\{\Psi^\dagger(x)[v_Fp\sigma_3+h+\Delta_r(x)\sigma_1-\Delta_i(x)\sigma_2]\Psi(x) + \Phi^\dagger(x)[-v_Fp\sigma_3+h+\Delta_r(x)\sigma_1 - \Delta_i(x)\sigma_2]\Phi(x)\} . \tag{2.6}$$

where we have rewritten ψ and ϕ as ψe^{ip_Fx} and ϕe^{-ip_Fx} to eliminate p_F from the kinetic energy terms. The self-

consistent equations are given by

$$\Delta_r(x)=-\tfrac{1}{2}g[\langle\Psi^\dagger(x)\sigma_1\Psi(x)\rangle+\langle\Phi^\dagger(x)\sigma_1\Phi(x)\rangle]\ ,$$
$$\Delta_i(x)=\tfrac{1}{2}g[\langle\Psi^\dagger(x)\sigma_2\Psi(x)\rangle+\langle\Phi^\dagger(x)\sigma_2\Phi(x)\rangle]\ , \tag{2.7}$$

where σ_i $(i=1,2,3)$ are usual Pauli matrices. In order to diagonalize the total Hamiltonian Eq. (2.6) we consider the following BdG equation:[20]

$$(v_Fp+h)u(x)+\Delta(x)v(x)=\epsilon u(x)\ ,$$
$$(-v_Fp+h)v(x)+\Delta^*(x)u(x)=\epsilon v(x) \tag{2.8a}$$

and

$$(-v_Fp+h)u'(x)+\Delta(x)v'(x)=\epsilon'u'(x)\ ,$$
$$(v_Fp+h)v'(x)+\Delta^*(x)u'(x)=\epsilon'v'(x)\ . \tag{2.8b}$$

By taking the complex conjugate of Eq. (2.8b) we can see that Eqs. (2.8a) and (2.8b) are equivalent when $\Delta(x)$ is real. In that case there also exists the following correspondence between the set of the eigenvalues ϵ_ν and eigenfunctions $u_\nu(x)$ and $v_\nu(x)$:

$$(\epsilon_\nu-h,u_\nu(x),v_\nu(x))\leftrightarrow(-(\epsilon_\nu-h),-v_\nu(x),u_\nu(x))\ .$$

Looking for a sinusoidal solution, we assume that $\Delta(x)$ is real in the following. Then the electron fields and Hamiltonian can be expressed in terms of $u_\nu(x)$ and $v_\nu(x)$ as

$$\Psi(x)=\sum_\nu\alpha_\nu\begin{bmatrix}u_\nu(x)\\v_\nu(x)\end{bmatrix}\ ,\quad \Phi(x)=\sum_\nu\beta_\nu\begin{bmatrix}u_\nu^*(x)\\v_\nu^*(x)\end{bmatrix}$$

and

$$\mathscr{H}=\sum_\nu\epsilon_\nu(\alpha_\nu^\dagger\alpha_\nu+\beta_\nu^\dagger\beta_\nu)$$

where the normalization condition of the eigenfunctions is given by

$$\int_0^L dx(|u_\nu(x)|^2+|v_\nu(x)|^2)=1$$

with L being the length of the system. The corresponding self-consistent equation (2.7) is reduced to

$$\Delta(x)=-g\sum_\nu[u_\nu(x)v_\nu^*(x)+v_\nu(x)u_\nu^*(x)]f(\epsilon_\nu)\ , \tag{2.9}$$

where $f(\epsilon_\nu)$ is the Fermi-distribution function.

It is convenient to introduce the quantities $\tilde{\epsilon}_\nu=\epsilon_\nu-h$, $\tilde{x}=x/v_F\hbar$, $\tilde{\partial}=\partial/\partial\tilde{x}$, and $U_v(x)=\binom{u_\nu(x)}{v_\nu(x)}$. We can rewrite Eqs. (2.8) and (2.9) as follows:

$$[-\sigma_3i\tilde{\partial}+\sigma_1\Delta(\tilde{x})]U_\nu(\tilde{x})=\tilde{\epsilon}_\nu U_\nu(\tilde{x})\ , \tag{2.10}$$
$$\Delta(\tilde{x})=-g\sum_\nu U_\nu^*(\tilde{x})\sigma_1U_\nu(\tilde{x})f(\epsilon_\nu)\ . \tag{2.11}$$

Making the transformation $F_\nu(x)\equiv\binom{f_{\nu-}(x)}{f_{\nu+}(x)}=TU_\nu(x)$ with $T=(1/\sqrt{2})(\sigma_2+\sigma_3)$, we finally obtain

$$[-\sigma_2i\tilde{\partial}-\sigma_1\Delta(\tilde{x})]F_\nu(\tilde{x})=\tilde{\epsilon}_\nu F_\nu(\tilde{x})\ , \tag{2.12}$$
$$\Delta(\tilde{x})=g\sum_\nu F_\nu^\dagger(\tilde{x})\sigma_1F_\nu(\tilde{x})f(\epsilon_\nu)\ . \tag{2.13}$$

Equation (2.12) is written as

$$[\tilde{\partial}^2+\epsilon_v^2-\Delta^2(\tilde{x})\pm\Delta'(\tilde{x})]f_{v\pm}(\tilde{x})=0\ , \tag{2.14}$$

where $\Delta'(\tilde{x})=d\Delta(\tilde{x})/d\tilde{x}$ and the normalization condition is

$$\int_0^L dx[|u_\nu(x)|^2+|v_\nu(x)|^2]=\hbar v_F\int_0^{L/v_F\hbar}d\tilde{x}F_\nu^\dagger(\tilde{x})F_\nu(\tilde{x})=1\ . \tag{2.15}$$

It is noted that the BdG equation [(2.12) or (2.14)] and the self-consistent equation (2.13) are merely those in the one-dimensional Peierls problem[21] where the exact solution has already been known.[17–19] Therefore, in the next section we briefly summarize the results obtained by these authors. We especially refer to the paper by Mertsching and Fischbeck.[18]

III. SELF-CONSISTENT SOLUTION

Suppose that the self-consistent solution of Eqs. (2.12) and (2.13) is given by

$$\Delta(\tilde{x})=\Delta_1k_1\mathrm{sn}(\Delta_1\tilde{x},k_1)\ , \tag{3.1}$$

where $\mathrm{sn}(\tilde{x},k)$ is the Jacobi elliptic function with modulus k. The two parameters Δ_1 and k_1 are to be determined self-consistently and characterize the superconducting state. With this solution Eq. (2.14) is transformed into

$$[\tilde{\partial}^2+\tilde{\epsilon}_\nu^2-Q(\tilde{x})]f_{\nu+}(\tilde{x})=0\ , \tag{3.2}$$
$$Q(\tilde{x})=\Delta^2(\tilde{x})-\Delta'(\tilde{x})\ . \tag{3.3}$$

It is not difficult to see[18] that Eq. (3.3) can be written in terms of the Weierstrass function[22] $\wp(\tilde{x})$ as

$$Q(x)=e_1+2\wp(\tilde{x}+\tilde{\omega}_3)\ , \tag{3.4}$$

where the three parameters associated with the Weierstrass function are given by

$$e_1=\tfrac{1}{6}\Delta_1^2(1+k_1^2)\ ,$$
$$e_2=-\tfrac{1}{12}\Delta_1^2(1-6k_1+k_1^2)\ , \tag{3.5}$$
$$e_3=-\tfrac{1}{12}\Delta_1^2(1+6k_1+k_1^2)\ .$$

The fundamental periodicities $2\tilde{\omega}_1$ and $2\tilde{\omega}_3$ of the elliptic function are

$$\tilde{\omega}_1=\frac{K(k)}{(e_1-e_3)^{1/2}}\ ,$$
$$\tilde{\omega}_3=\frac{iK(k')}{(e_1-e_3)^{1/2}}\ , \tag{3.6}$$

and the modulus k and complementary modulus k' are given by

$$k^2=\frac{e_2-e_3}{e_1-e_3}\ ,$$
$$k'^2=1-k^2 \tag{3.7}$$

with $K(k)$ being the complete elliptic integral of the first kind. We have used the same notation for the periodicity

ω_i for x. Therefore, the eigenvalue equation (3.2) is reduced to solving the Lamé equation:[22]

$$[\tilde{\partial}^2+\tilde{\epsilon}_\nu^2-e_1-2\wp(\tilde{x}+\tilde{\omega}_3)]f_{\nu+}(\tilde{x})=0\ . \tag{3.8}$$

This is merely the one-dimensional Bloch problem in a periodic potential. It is known[22] that the periodic solution of this Lamé equation is given by

$$f_{\nu+}(\tilde{x})=\left[\frac{\wp(\tilde{x}+\tilde{\omega}_3)-e}{2L(\bar{\wp}-e)}\right]^{1/2} \times\exp\left[iC(\tilde{\epsilon})\int_0^{\tilde{x}}\frac{dx'}{\wp(x'+\tilde{\omega}_3)-e}\right] \tag{3.9}$$

with the proper normalization,[18] where

$$e=e_1-\tilde{\epsilon}_\nu^2\ , \tag{3.10}$$

$$C(\epsilon)=\pm\epsilon[(\epsilon^2-\epsilon_2^2)(\epsilon^2-\epsilon_3^2)]^{1/2}\ , \tag{3.11}$$

$$\epsilon_i^2=e_1-e_i\quad (i=2\text{ or }3)\ , \tag{3.12}$$

$$\bar{\wp}=\frac{1}{\tilde{\omega}_1}\int_0^{\tilde{\omega}_1}dx\,\wp(x+\tilde{\omega}_3)=e_1-(e_1-e_3)\frac{E(k)}{K(k)}\ , \tag{3.13}$$

with $E(k)$ being the complete elliptic integral of the second kind. Note that for $\tilde{\epsilon}_2^2<\tilde{\epsilon}_\nu^2<\tilde{\epsilon}_3^2$, $C(\tilde{\epsilon})$ becomes complex, meaning that energy gaps appear in the spectrum.

By applying the Bloch theorem $f_{\nu+}(\tilde{x}+2\tilde{\omega}_1)=e^{2i\tilde{q}\tilde{\omega}_1}f_{\nu+}(\tilde{x})$, we can determine the $v_F\hbar$ times wave number $\tilde{q}$ as

$$\tilde{q}(\epsilon)=\hbar v_F q(\epsilon) =\pm\frac{1}{K(k)}\left[\frac{(e_1-e)(e_2-e)}{e_3-e}\right]^{1/2}\Pi\left[\frac{e_2-e_3}{e_3-e},k\right]\ , \tag{3.14}$$

where $\Pi(\rho,k)$ is the complete elliptic integral of the third kind. The density of states $N(\epsilon)$ is derived through $N(\epsilon)=1/\pi\,|\,dq/d\epsilon\,|$ as

$$N(\epsilon)=\frac{1}{\pi\hbar v_F}\frac{|\tilde{\epsilon}^2+\bar{\wp}-e_1|}{[(\tilde{\epsilon}^2-\delta^2)(\tilde{\epsilon}^2-k'^2\delta^2)]^{1/2}} \times\Theta((\tilde{\epsilon}^2-\delta^2)(\tilde{\epsilon}^2-k'^2\delta^2))\ , \tag{3.15}$$

where we have introduced the parameter δ defined by

$$\delta^2=e_1-e_3 \tag{3.16}$$

and the step function $\Theta(x)$. Thus we obtain $e_1-e_2=k'^2\delta^2$ and $e_2-e_3=k^2\delta^2$. The density of states $N(\epsilon)$ in Eq. (3.15) clearly indicates the two-energy-gap structure in the spectrum: One corresponds to 2δ and the other to $2(1-k')\delta$, as will be seen later in detail. The two independent parameters k_1 and Δ_1 introduced earlier can now be related to the newly defined parameters k and δ through

$$\Delta_1=(1+k')\delta\ ,\qquad k_1=\frac{1-k'}{1+k'}\ . \tag{3.17}$$

The latter is known as the Landen transformation.[22]

In order to determine the two unknown parameters k and δ of the problem let us first consider the self-consistent Eq. (2.13):

$$\Delta(\tilde{x})=g\sum_\nu[f_{\nu+}^*(\tilde{x})f_{\nu-}(\tilde{x})+f_{\nu-}^*(\tilde{x})f_{\nu+}(\tilde{x})]f(\epsilon_\nu) =-g\sum_\nu\frac{f(\epsilon_\nu)}{\tilde{\epsilon}_\nu}[\tilde{\partial}+2\Delta(\tilde{x})]f_{\nu+}^*(\tilde{x})f_{\nu+}(\tilde{x})\ , \tag{3.18}$$

where we have used Eq. (2.12). Substituting Eq. (3.9) into Eq. (3.18) we obtain after some manipulations

$$\frac{1}{g}=-\frac{1}{L}\sum_\nu\frac{f(\epsilon_\nu)\tilde{\epsilon}_\nu}{\bar{\wp}-e_1+\tilde{\epsilon}_\nu^2}\ , \tag{3.19}$$

which yields the following form by utilizing Eq. (3.15):

$$\ln\frac{\delta_0}{k\delta}=\int_\delta^\infty[f(\epsilon+h)+f(\epsilon-h)]\frac{\epsilon\,d\epsilon}{[(\epsilon^2-\delta^2)(\epsilon^2-k'^2\delta^2)]^{1/2}}+\int_0^{k'\delta}[f(h-\epsilon)-f(h+\epsilon)]\frac{\epsilon\,d\epsilon}{[(\epsilon^2-\delta^2)(\epsilon^2-k'^2\delta^2)]^{1/2}}\ . \tag{3.20}$$

The order parameter at $h=0$ and $T=0$ is introduced by $\delta_0=2\tilde{q}_s e^{-1/gN(0)}$ where $N(0)=1/\pi v_F\hbar$ and $\tilde{q}_s$ is the momentum cutoff.

The free energy Ω per unit length is expressed as

$$\Omega=-\frac{2}{\beta L}\sum_q\ln(1+e^{-\beta\epsilon_q})+\frac{1}{gL}\int_0^L\Delta^2(x)dx\ , \tag{3.21}$$

which is explicitly evaluated as

$$\Omega=-\frac{1}{\pi\hbar v_F}\left\{\tilde{q}_s(\tilde{q}_s+2h)+\frac{\pi h\delta}{K(k)}+\delta^2\left[\left[1+k'^2-2\frac{E(k)}{K(k)}\right]\left[\ln\frac{\delta_0}{k\delta}+1\right]-\frac{1+k'^2}{2}\right]\right\} +\frac{1}{\hbar v_F}\frac{\delta}{\beta K(k)}\ln\frac{(1+e^{-\beta(\delta+h)})(1+e^{-\beta(\delta-h)})}{(1+e^{-\beta(h-k'\delta)})(1+e^{-\beta(h+k'\delta)})}+\frac{2}{\pi}\int_0^{k'\delta}[f(h-\epsilon)-f(h+\epsilon)]q(\epsilon)d\epsilon -\frac{2}{\pi}\int_\delta^\infty[f(\epsilon+h)+f(\epsilon-h)]q(\epsilon)d\epsilon\ , \tag{3.22}$$

where we have used Eqs. (3.15) and (3.20). Minimizing Ω with respect to k or δ yields

$$\frac{\partial\Omega}{\partial\delta}=\frac{1}{\hbar v_F K(k)}F(T,h,\delta,k')=0\ , \tag{3.23}$$

$$\begin{aligned}F(T,h,\delta,k')=&-h+\frac{2}{\pi}\delta E(k)+\frac{1}{\beta}\ln\frac{(1+e^{-\beta(\delta+h)})(1+e^{-\beta(\delta-h)})}{(1+e^{-\beta(h-k'\delta)})(1+e^{-\beta(h+k'\delta)})}\\&+\frac{2}{\pi}\int_0^{k'\delta}[f(h-\delta)-f(h+\delta)]\left[S\left[\sin^{-1}\frac{\epsilon}{k'\delta},k\right]+\epsilon\delta\frac{E(k)-(1+k'^2-\epsilon^2/\delta^2)K(k)}{[(\delta^2-\epsilon^2)(k'^2\delta^2-\epsilon^2)]^{1/2}}\right]d\epsilon\\&-\frac{2}{\pi}\int_\delta^\infty[f(\epsilon+h)-f(\epsilon-h)]\left[S\left[\sin^{-1}\frac{\delta}{\epsilon},k\right]-\epsilon\delta\frac{E(k)-(k'^2\delta^2/\epsilon^2)K(k)}{[(\epsilon^2-\delta^2)(\epsilon^2-k'^2\delta^2)]^{1/2}}\right]d\epsilon\ ,\end{aligned} \tag{3.24}$$

where the Heumann function $S(\phi,k)$ is introduced by

$$S(\phi,k)=[E(k)-K(k)]F(\phi,k')+K(k)E(\phi,k')\ , \tag{3.25}$$

$F(\phi,k')$ and $E(\phi,k')$ are the incomplete elliptic integrals of the first and second kind. Equations (3.20) and (3.24) constitute a complete set of the simultaneous equations for determining the two parameters k and δ.

It is easy to see that at $T=0$ the solution of Eqs. (3.20) and (3.24) is given by

$$\delta=\frac{\delta_0}{k}\ , \tag{3.26}$$

$$h=\frac{2}{\pi}\delta E(k)\ . \tag{3.27}$$

Since $1\le E(k)\le\pi/2$ for $0\le k\le 1$ then δ is always greater than or equal to δ_0. At finite temperatures we must solve these equations numerically.

IV. PHYSICAL PROPERTIES OF THE SELF-CONSISTENT SOLUTION

A. Phase diagram

Let us consider the phase diagram in the T-vs-h plane. (We use energy units for the temperature T). From Eq. (3.1) or equivalently from

$$\Delta(\tilde{x})=\delta(1-k')\mathrm{sn}((1+k')\delta\tilde{x},k_1)\ , \tag{4.1a}$$

it is seen that the solution with $k=1$ corresponds to the ordinary BCS state characterized by the spatially homogeneous order parameter, $\Delta(x)=\delta$, while the snoidal solution with $k\neq 1$ (we call it the sn phase hereafter) corresponds to the spatially modulated superconducting state whose wave number is

$$\tilde{q}=\frac{\pi\delta}{K(k)} \tag{4.1b}$$

and the amplitude of the order parameter $\Delta(x)$ is $\delta(1-k')$. When $k\to 0$, $\Delta(x)$ approaches sinusoidal modulation. The order parameter δ in the BCS state is evaluated by setting $k=1$ in Eq. (3.20), that is,

$$\ln\frac{\delta_0}{\delta}=\int_\delta^\infty[f(\epsilon+h)+f(\epsilon-h)]\frac{1}{(\epsilon^2-\delta^2)^{1/2}}d\epsilon\ . \tag{4.2}$$

This is merely the formula given by Maki and Tsuneto,[23] who first considered the Pauli paramagnetic effect on superconductivity. The boundary line T_c between the normal and BCS state is determined by taking $\delta\to 0$ and $T\to T_c$:

$$\ln\frac{T_{c0}}{T_c}+\mathrm{Re}\left[\psi(\tfrac{1}{2})-\psi\left[\frac{1}{2}+\frac{ih}{2\pi T_c}\right]\right]=0 \tag{4.3}$$

with $T_{c0}=(\gamma/\pi)\delta_0$ ($\ln\gamma$ is the Euler constant). The digamma function is denoted by $\psi(x)$.

The phase boundary between the normal and sn state is determined by setting $k=0$ in Eq. (3.19), that is

$$\begin{aligned}\frac{\pi}{g}&=-\frac{\pi}{L}\sum_q\frac{f(\epsilon_q)(\epsilon_q+h)}{(\epsilon_q+h)^2+\bar{\varphi}-e_1}\\&=-\frac{1}{\hbar v_F}\int_0^{\tilde{q}_s}d\epsilon[f(\epsilon-h)-f(-\epsilon-h)]\frac{\epsilon}{\epsilon^2-\delta^2}\ .\end{aligned} \tag{4.4}$$

After some manipulations we obtain

$$\ln\frac{T_{c0}}{T_c}+\mathrm{Re}\left[\psi(\tfrac{1}{2})-\tfrac{1}{2}\psi\left[\frac{1}{2}+\frac{\delta+h}{2\pi T_c}i\right]-\tfrac{1}{2}\psi\left[\frac{1}{2}-\frac{\delta-h}{2\pi T_c}i\right]\right]=0\ . \tag{4.5}$$

We note that 2δ corresponds to the wave number of the sn phase when $k\to 0$ as is seen from Eq. (4.1b) and $\Delta(\tilde{x})\propto\sin(2\delta\tilde{x})$ near the boundary. In order to determine δ on the boundary line T_c we impose the condition that the transition temperatre T_c be maximized with respect to δ, that is, $dT_c/d\delta=0$, yielding

$$\mathrm{Im}\left[\psi'\left[\frac{1}{2}+\frac{\delta+h}{2\pi T_c}i\right]-\psi'\left[\frac{1}{2}-\frac{\delta-h}{2\pi T_c}i\right]\right]=0\ . \tag{4.6}$$

Equations (4.5) and (4.6) coincide with those in the previous work.[24] We can show that $T_c\propto h^{-1}$ when h becomes large. This asymptotic behavior of T_c is characteristic of the one-dimensional model[18,24] and different from that of the three-dimensional case.[13–15] In the latter case there is a finite critical field at $T=0$ beyond which the superconductivity ceases to exist.

The phase boundary line between the BCS ($k=1$) and the sn phase ($k\neq 1$) is determined by taking the limit $k\to 1$ and $\delta\to\delta_c$ in Eqs. (3.20) and (3.23), that is, $F(T,h,\delta_c,k'\to 0)=0$, or

$$-h+\frac{2}{\pi}\delta_c+\frac{1}{\beta}\ln\frac{(1+e^{-\beta(\delta_c+h)})(1+e^{-\beta(\delta_c-h)})}{(1+e^{-\beta h})^2}-\frac{2}{\pi}\int_{\delta_c}^{\infty}[f(\epsilon+h)-f(\epsilon-h)]\left[\sin^{-1}\frac{\delta_c}{\epsilon}-\frac{\delta_c}{(\epsilon^2-\delta_c^2)^{1/2}}\right]d\epsilon=0\ . \quad (4.7)$$

At $T=0$ from Eqs. (3.26) and (3.27) this boundary is given by the critical field $h_{\rm cr}=(2/\pi)\delta_0$.

The phase diagram determined by solving Eqs. (4.3) and (4.5)—(4.7) numerically is depicted in Fig. 1. The three second-order phase-transition lines meet at a point called the Leung point.[24]

So far we only considered the real solution of the BdG equation. There also exists a complex solution described by $\Delta(x)=\Delta_0 e^{iqx}$, the helical solution. This has been investigated by Fulde and Ferrell[13] and Takada and Izuyama.[15] We show the calculation of the helical solution in the Appendix. It is seen that the phase transition from the BCS to the helical phase is first order, in agreement with the three-dimensional spherical Fermi-surface model,[13–15] and that the critical field ($h_{\rm cr}=0.68\delta_0$) at $T=0$ between the BCS and the helical phase is greater than that between the BCS and the sn phase case [$h_{\rm cr}=(2/\pi)\delta_0$], implying that the sn phase is more stable than the helical solution in the T vs h plane. Physically this is true because the soliton lattice structure gives energy gaps right at the Fermi level, leading to a reduced total energy. Hereafter we only consider the sn phase.

B. Energy-gap structure

One of the most distinctive characteristics of the sn phase is the two-energy-gap structure. As shown in Eq. (3.15) and Fig. 2, there exist the two energy gaps, and at the gap edges the density of states has a square-root singularity. The midgap state is a salient feature of the spatially modulated order parameter incommensurate with the underlying crystal lattice structure. In Fig. 2 we depict the variation of the edge of the two energy gaps as a function of the modulus k where $k=1$ corresponds to the BCS state with a single energy gap δ_0 and near $k\simeq 1$, there appears a so-called soliton midgap level which rapidly spreads and fills the gap as k becomes small. The purely sinusoidally modulated phase corresponds to the $k=0$ limit and only appears right on the boundary line.

C. Order parameter

In this section we present numerical results of the solution of Eqs. (3.20) and (3.23) for the two parameters δ and k which completely determine the order parameter $\Delta(\tilde{x})$ in Eq. (4.1). Let us first study the two limiting behaviors of $\Delta(\tilde{x})$ at $T=0$ when h is large and h approaches $h_{\rm cr}=(2/\pi)\delta_0$.

1. $h\to\infty$. As $h\to\infty$ we can see from Eqs. (3.26) and (3.27) that $k\to 1/h$ and $\delta\to h$. Hence the amplitude $\delta(1-k')$ of $\Delta(\tilde{x})$ tends to $1/2h$ and the wave number $\tilde{q}$ becomes $2h$.

2. $h/\delta_0\to\pi/2+0$. We set $h/\delta_0=2/\pi+\Delta h/\delta_0$ ($\Delta h>0$). Knowing the asymptotic behavior of $E(k)$, that $E(k)\simeq 1+\frac{1}{2}k'^2\ln(4/k')$, we obtain from Eq. (3.27) that $\tilde{q}\simeq\delta_0/\ln(\delta_0/\Delta h)$.

We plot several numerical results in Figs. 3—10. Figure 3 illustrates the variation of the amplitude $\delta(1-k')$ of $\Delta(\tilde{x})$ along the boundary line between the BCS and the sn phase. The variation of the wave number $\tilde{q}$ along the transition-temperature line of the sn phase is depicted in Fig. 4. In Figs. 5 and 6 we show the changes of the wave number and amplitude at a fixed temperature $T/\delta_0=0.12$. Another set of figures, 7 and 8, illustrates the changes of the wave number and amplitude at a fixed field $h/\delta_0=0.8$. The overall features of the wave number and amplitude are depicted stereographically in Figs. 9 and 10.

V. CONDUCTION-ELECTRON SPIN POLARIZATION

It is important to realize that the sn phase stabilized under a high-molecular-field region is accompanied inevitably and automatically by spin polarization of the conduction electron, which includes both spatially uniform and spatially modulated components with wave number $2q$, twice the fundamental wave number of the order parameter. (The helical phase is also magnetically polarized without the spatially modulated component.) We define

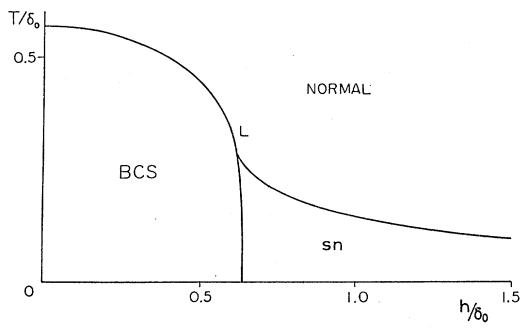

FIG. 1. Phase diagram in the temperature (T) vs field (h). All of the three lines are the second-order phase-transition lines and meet at the point L. T and h are normalized by δ_0.

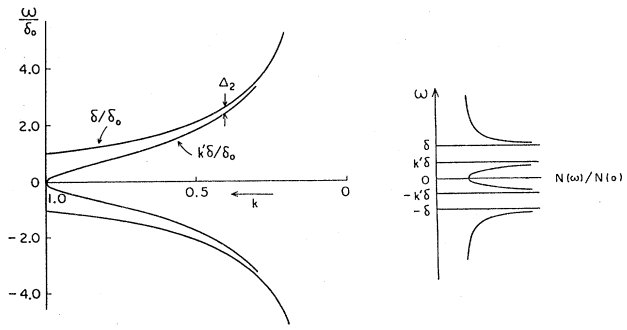

FIG. 2. Energy-gap edges as a function of the modulus k where $k=1$ corresponds to the BCS state and $k\neq 1$ to the sn state. An inset shows a schematic density of states in the sn state.

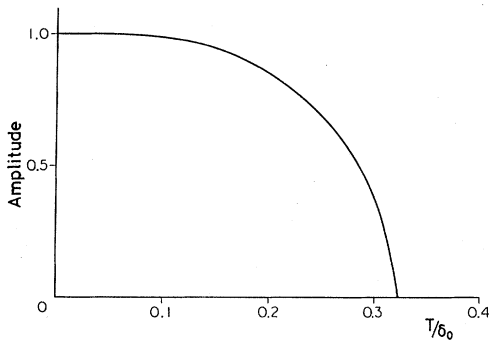

FIG. 3. Amplitude $\delta(1-k')/\delta_0$ of the order parameter as a function of temperature along the boundary line between the BCS and sn state.

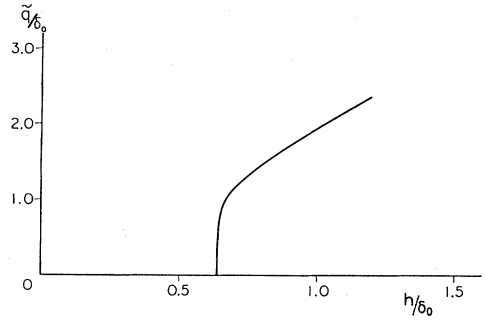

FIG. 5. Wave number $\tilde{q}/\delta_0$ as a function of h/δ_0 at a constant temperature $T/\delta_0=0.12$.

the spin polarization $S(x)$ of the conduction electrons at a point x as

$$S(x)=\langle \psi_\uparrow^\dagger(x)\psi_\uparrow(x)-\psi_\downarrow^\dagger(x)\psi_\downarrow(x) +\phi_\uparrow^\dagger(x)\phi_\uparrow(x)-\phi_\downarrow^\dagger(x)\phi_\downarrow(x)\rangle \ . \tag{5.1}$$

This can be written in terms of the eigenfunctions $f_{\nu\pm}(x)$ of the BdG Eq. (2.14) as

$$S(\tilde{x})=2\sum_\nu [f(\epsilon_\nu)-\tfrac{1}{2}][\,|f_{\nu+}(\tilde{x})|^2+|f_{\nu-}(\tilde{x})|^2] \ . \tag{5.2}$$

It is easily proved that $|f_{\nu-}(\tilde{x})|^2=|f_{\nu+}(\tilde{x}+\tilde{\omega}_1)|^2$ using Eq. (2.12) and noting that $Q(\tilde{x}+\tilde{\omega}_1)=\Delta^2(\tilde{x})+\Delta'(\tilde{x})$. Substituting Eq. (3.9) into Eq. (5.2) we obtain

$$S(\tilde{x})=\frac{1}{L}\sum_\nu [f(\epsilon_\nu)-\tfrac{1}{2}]\frac{\wp(\tilde{x}+\tilde{\omega}_3)+\wp(\tilde{x}+\tilde{\omega}_1+\tilde{\omega}_3)-2e}{\bar{\wp}-e} \ . \tag{5.3}$$

Using the following relation[22]

$$\wp(\tilde{x}+\tilde{\omega}_3)=e_3+\delta^2k^2\mathrm{sn}^2(\delta\tilde{x},k) \ , \tag{5.4}$$

we obtain

$$S(\tilde{x})=2S_0+2k^2\delta^2S_1[\mathrm{sn}^2(\delta\tilde{x},k)+\mathrm{sn}^2(\delta\tilde{x}+\delta\tilde{\omega}_1,k)] \ , \tag{5.5}$$

where

$$S_0=\frac{1}{\pi\hbar v_F}\int_0^{k'\delta} d\epsilon[f(\epsilon+h)-f(\epsilon-h)]\left[\frac{\delta^2-\epsilon^2}{k'^2\delta^2-\epsilon^2}\right]^{1/2}+\frac{1}{\pi\hbar v_F}\int_\delta^\infty d\epsilon[f(\epsilon+h)-f(\epsilon-h)]\left[\frac{\epsilon^2-\delta^2}{\epsilon^2-k'^2\delta^2}\right]^{1/2} , \tag{5.6}$$

$$S_1=-\frac{1}{2\pi\hbar v_F}\int_0^{k'\delta} d\epsilon[f(\epsilon+h)-f(\epsilon-h)]\frac{1}{[(\epsilon^2-\delta^2)(\epsilon^2-k'^2\delta^2)]^{1/2}} +\frac{1}{2\pi\hbar v_F}\int_\delta^\infty d\epsilon[f(\epsilon+h)-f(\epsilon-h)]\frac{1}{[(\epsilon^2-\delta^2)(\epsilon^2-k'^2\delta^2)]^{1/2}} \ . \tag{5.7}$$

Since the Fourier decomposition of the Jacobi elliptic function is given by

$$k^2[\mathrm{sn}^2(\delta\tilde{x},k)+\mathrm{sn}^2(\delta\tilde{x}+\delta\tilde{\omega}_1,k)]=2\left[1-\frac{E}{K}-\frac{\pi^2}{K^2}\sum_{n=1}^\infty \frac{2n\cos(2\pi n\delta\tilde{x}/K)}{\sinh(2\pi nK'/K)}\right] , \tag{5.8}$$

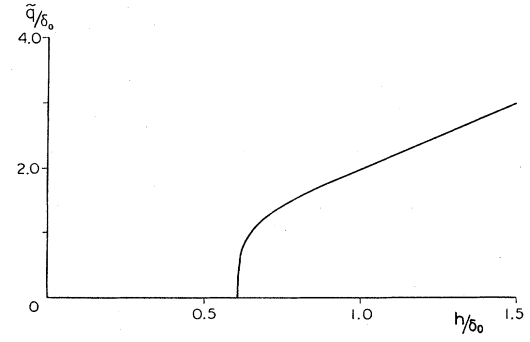

FIG. 4. Wave number $\tilde{q}/\delta_0$ as a function of the field h along the transition line between the normal and sn phase.

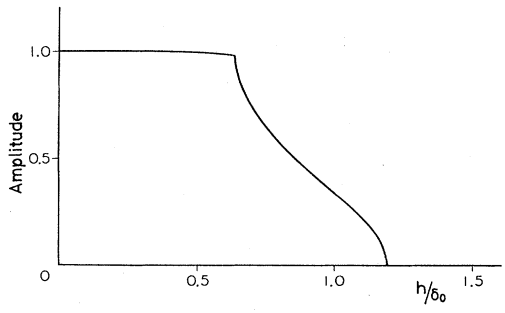

FIG. 6. Amplitude $\delta(1-k')/\delta_0$ of the order parameter as a function of h/δ_0 at a constant temperature $T/\delta_0=0.12$.

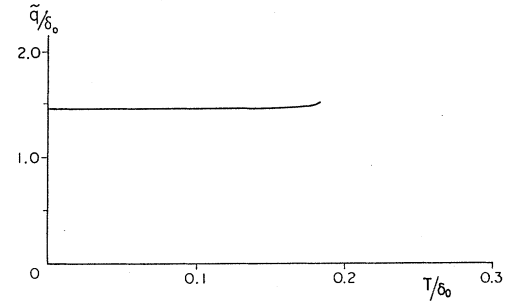

FIG. 7. Wave number $\tilde{q}/\delta_0$ as a function of T/δ_0 at a constant field $h/\delta_0=0.8$.

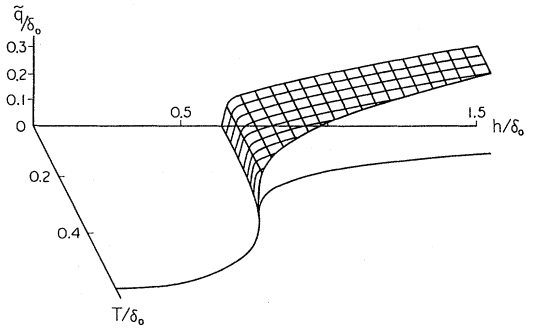

FIG. 9. Stereograph of the wave number $\tilde{q}/\delta_0$ in the T vs h plane.

where $K\equiv K(k)$, $K'\equiv K(k')$, then $E\equiv E(k)$, then Eq. (5.5) becomes

$$S(\tilde{x})=2S_0+4S_1\delta^2\left[1-\frac{E}{K}-\frac{\pi^2}{K^2}\sum_{n=1}^{\infty}\frac{2n\cos(2\pi n\delta\tilde{x}/K)}{\sinh(2\pi nK'/K)}\right]. \tag{5.9}$$

At zero temperature this expression is considerably simplified, that is, Eqs. (5.6) and (5.7) become

$$S_0=-\frac{\delta}{\pi\hbar v_F}E',\quad S_1=\frac{K'}{2\pi\hbar v_F\delta}. \tag{5.10}$$

Thus Eq. (5.9) is reduced to

$$\frac{S(\tilde{x})}{\delta_0}=\frac{1}{\hbar v_F kK}\left[1-\sum_{n=1}^{\infty}\frac{2kK'\tilde{q}_n/\delta_0}{\sinh(kK'\tilde{q}_n/\delta_0)}\cos(\tilde{q}_n\tilde{x})\right] \tag{5.11}$$

with $\tilde{q}_n\equiv 2\pi n\delta_0/kK$. In the limit of $k\to 0$ we obtain

$$S(\tilde{x})=-\chi_P h-\frac{8\delta_0 k^3}{\pi\hbar v_F}\ln\left[\frac{1}{k}\right]\cos(4h\tilde{x}), \tag{5.12}$$

where the Pauli susceptibility χ_P is given by $\chi_P=2N(0)$ and the density of states $N(0)$ at the Fermi level is $1/\pi v_F\hbar$. Near the boundary between the normal and the sn phase the uniform component becomes continuously that of the normal electron described by the Pauli susceptibility. On the other hand, in the limit of $k\to 1$, the asymptotic form of Eq. (5.9) is

$$S(\tilde{x})=-\frac{\delta_0}{2\hbar v_F}[1-\tanh^2(\delta_0\tilde{x})]. \tag{5.13}$$

This clearly indicates that the spin polarization is carried by the kinks of the order parameter $\Delta(\tilde{x})$ where the amplitude of the superconducting state vanishes.

We perform numerical calculations of Eq. (5.5) to obtain the spatial dependences of the spin polarization $S(\tilde{x})$. We plot some examples of the results in Figs. 11 and 12 where the spatial dependences of the order parameter $\Delta(\tilde{x})$ are also displayed. Figure 13 illustrates the histogram of the Fourier components of $S(\tilde{q}_n)$ in the h versus $\tilde{q}$ plane at a constant temperature $T/\delta_0=0.12$. This indicates that the position of the fundamental component ($n=1$) does not appreciably change as h increases except a narrow region near $h_{cr}=(2/\pi)\delta_0$, and in that critical region many higher harmonics appear, rapidly diminishing in higher fields. Figure 14 exhibits the field dependence of the fundamental component ($n=1$) in Eq. (5.9).

VI. INTERPRETATION OF EXPERIMENTS ON $ErRh_4B_4$

Let us apply the above theory to experiments on ERB, especially the neutron experiment by Sinha *et al.*[2] Al-

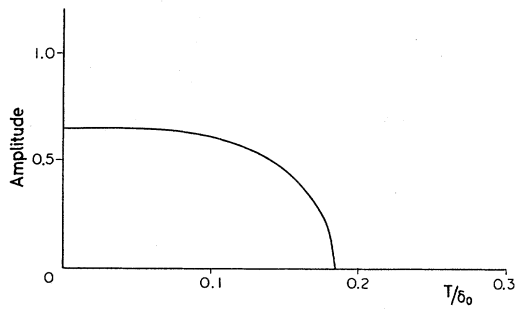

FIG. 8. Amplitude $\delta(1-k')/\delta_0$ of the order parameter as a function of T/δ_0 at a constant field $h/\delta_0=0.8$.

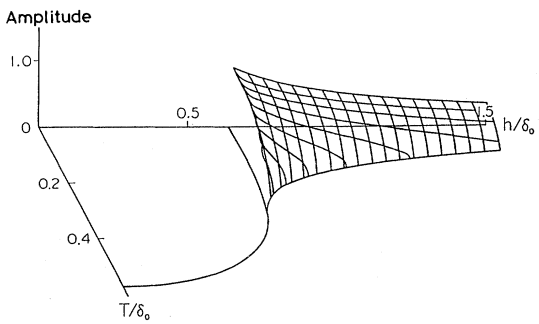

FIG. 10. Stereograph of the amplitude $\delta(1-k')/\delta_0$ in the T vs h plane.

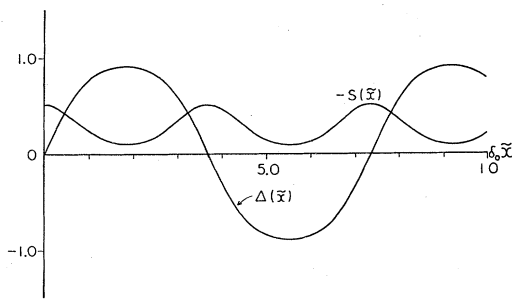

FIG. 11. Variation of the order parameter $\Delta(\tilde{x})/\delta_0$ and the spin polarization $\hbar v_F S(\tilde{x})/\delta_0$ in the case of $h/\delta_0=0.65$ and $T=0$.

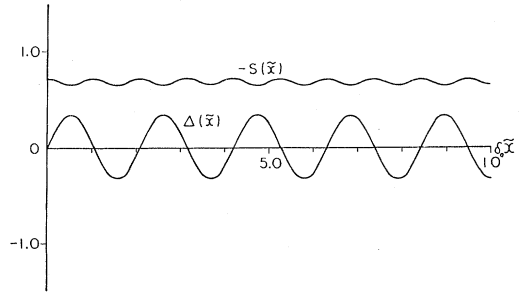

FIG. 12. Variation of the order parameter $\Delta(\tilde{x})/\delta_0$ and the spin polarization $\hbar v_F S(\tilde{x})/\delta_0$ in the case of $h/\delta_0=1.5$ and $T=0$.

though the other ferromagnetic superconductor HMS exhibits essentially the same phenomena as in ERB, we must wait to apply it to HMS because the persistence[4] of a large residual satellite scattering intensity at lower temperatures may indicate that neutron experiments must be improved. Thus we mainly consider ERB in the following.

A. Strength of the ferromagnetic molecular field

The ferromagnetic molecular field $H_{\rm ex}$ arising from the sf exchange interaction Eq. (2.2) is given by $H_{\rm ex}(T)=(I/2)(g_J-1)[M(T)/g_e\mu_B]$ which is temperature dependent through the magnetization $M(T)=\langle J_z\rangle$: the thermal average of the $4f$ total angular momentum J. g_e is the gyromagnetic ratio and μ_B is the Bohr magneton. Taking the value of the exchange integral $I\cong 2.7\times 10^{-2}$ eV estimated by us[25] for the rare-earth rhodium boride compounds $R{\rm Rh}_4{\rm B}_4$ and the free-ion value ($g_J=\frac{6}{5}$, $J=7.5\mu_B$) for the Er ion, we obtain $H_{\rm ex}\simeq 400$ kG. On the other hand, the order of magnitude of the molecular field at which the sn phase is stabilized is determined by the critical field $h_{\rm cr}=(2/\pi)\delta_0$. This is of the same order of the Chandrasekhar-Clogston limiting field H_p ($=\delta_0/\sqrt{2}\mu_B$), which is of the order of $H_p\simeq 160$ kG for ERB when taking $T_{c1}=8.7$ K. These rough estimates indicate that there should exist a narrow temperature region where the sn phase is stabilized below the ferromagnetic transition temperature $T_M\simeq 1.2$ K.

B. Successive phase transitions

Upon decreasing the temperature the BCS state appears at $T=T_{c1}$ and continuously transforms into the sn state at $T=T_{\rm sn}$ which corresponds to the critical field $h_{\rm cr}=(2/\pi)\delta_0$ immediately after the $4f$ moment system begins to order ferromagnetically at T_M. The phase transition at $T=T_{\rm sn}$ is of second order according to the present theory. This coincides with the neutron experiment[2] reporting that the satellite intensity continuously grows. As the temperature further decreases the ferromagnetic magnetization rapidly grows and exceeds the value of the upper critical molecular field at $T=T_{c2}$ beyond which the sn state ceases to exist. This reentrant phase transition from the sn state to the normal ferromagnetic state should be of second order according to the present theory, which considers only the conduction-electron system and regards the $4f$ moment system as an external entity. However, if we take into account the reaction of the $4f$ system due to the formation of the sn state, this reentrant phase transition becomes first order as explained in a previous paper.[11] In fact, the upper critical field H_{c2} measurement on ERB by Crabtree *et al.*,[26] who found the first-order transition when an external field is applied parallel to the easy axis of the magnetization, is interpreted successfully by this idea.[27]

C. Sinusoidally modulated magnetic phase

The sinusoidally modulated magnetic phase observed in the neutron experiment as satellite peaks is characterized by the wavelength 100 Å independent of temperature.[2] As already shown previously[10] the wave number q of the sn phase is roughly estimated by $q\cong p_F h\bar{q}/\epsilon_F$ where $\bar{q}$ is of the order of unity. Since the energy associated with the molecular field is $\sim\mu_B H_{\rm ex}$ ($\simeq 10^{-3}$ eV) and the Fermi energy ϵ_F and wave number k_F are estimated as $\epsilon_F^{-1}\sim 1$ eV^{-1} and $k_F\simeq 1$ Å^{-1}, respectively, we obtain $q\simeq O(10^{-2}$–10^{-3} Å$^{-1})$ which is within the range of the experimental value ($q\sim 0.06$ Å^{-1}). A similar estimate[10] of q gives a correct order of magnitude for HMS.

According to the present theory the periodicity of the conduction-electron polarization $S(x)$ associated with $\Delta(x)$ depends on the field h, in other words, the temperature in the context of the experimental situation. As seen from Fig. 13 the region where the periodicity rapidly varies is very narrowly limited near the onset field of the sn state. Therefore, except for the narrow temperature region near $T_{\rm sn}$, the temperature dependence of the periodicity is very weak, in agreement with the experiment.[2,3] In this connection an interesting fact is reported by Sinha and Kjems[28] that at $T=1.0$ K they observe a peak with a wave number much smaller than that of the satellite fully established at $T\simeq 0.7$ K. This finding might be related to our assertion that the periodicity of the spin modulation should change continuously. We expect that the satellites associated with many higher harmonics should appear in this temperature region near $T_M=1.2$ K. However, the wave number becomes very small, as seen from Fig. 5 and higher satellites merge toward the center, $q=0$, and thus cannot be observed readily because the ferromagnetic

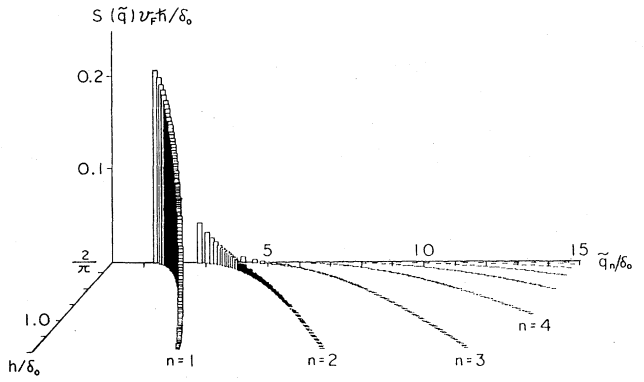

FIG. 13. Histogram $\hbar v_F S(\tilde{q}_n)/\delta_0$ of the Fourier components ($n=1,2,3,\ldots$) of the spin polarization in the $\tilde{q}_n/\delta_0$ vs h plane at $T/\delta_0=0.12$. We have omitted the part immediately near the origin for clarity.

component situated at $q=0$ might obscure these fine structures around the center, and also because the intensities of harmonics are weak. In spite of this difficulty we think that it is important to observe the higher-harmonic satellites associated with the distorted sinusoidal modulation or the soliton lattice structure, keeping temperatures just below $T_M=1.2$ K.

The temperature dependence of the satellite intensity in ERB is a decreasing function of temperature. On the other hand, the amplitude of the spin modulation in the sn state decreases upon increasing h as displayed in Figs. 13 and 14. This is in contrast to the experiment. We emphasize here that the satellite scattering mainly arises from the $4f$ moment system and the conduction-electron spin modulation only triggers the modulated moment structure of the $4f$ system through the sf exchange interaction. Along the line developed in the present theory we gave an explanation[11] of the observed temperature dependence of the satellite intensity by using a phenomenological Ginzburg-Landau theory.

VII. SUMMARY AND DISCUSSION

We have obtained the exact solution within the mean-field approximation of the one-dimensional problem on the superconductivity under a ferromagnetic molecular field. Differing from the previous theory[13] which considers only the fundamental wave number, we take into account the effect of infinite numbers of higher harmonics, which is important near the second-order transition line between the BCS and the sn state. In a high-field region the superconducting state with a spatially varying order parameter $\Delta(x)$ is found to be stable over the BCS state. The spatial dependence of this state is not a simple sinusoidal form but a distorted wave form or soliton lattice structure (so-called discommensuration structure). We have evaluated the temperature and field dependences of the amplitude and periodicity of the order parameter and calculated the spin polarization of the conduction electrons. We have also examined the helical solution[14,15] which turns out to be metastable compared with the sn solution.

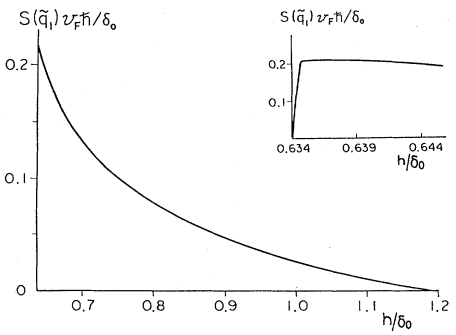

FIG. 14. Field dependence of the fundamental Fourier component $\hbar v_F S(\tilde{q}_1)/\delta_0$ at $T/\delta_0=0.12$. The inset shows the figure in the low-field region.

The general feature of various experiments on $ErRh_4B_4$ is consistent with the present theory: Namely, the sinusoidally modulated phase observed by neutron experiments as satellites is interepreted in terms of the sn phase. The order of magnitude of the periodicity of the magnetic modulated state and its temperature dependence have been also explained.

Although for mathematical convenience we have employed a one-dimensional band model, it turns out that this leads to the essentially similar physical results[13–15] based on a three-dimensional Fermi-sphere model. We may justify its application to $ErRh_4B_4$ which has a three-dimensional band structure for the following reason: It is noted that the observed sinusoidally modulated phase is characterized by a single wave vector directed to 45° from the a axis in the ac plane of the tetragonal crystal. Theoretically, the wave vector of the spatial modulation is chosen so as to satisfy a nesting condition for the spin-up and -down bands. Hence after transforming into the modulated phase the resulting electronic band structure along the direction of the chosen wave vector might be one-dimensional-like.

We have neglected the so-called electromagnetic interaction which leads to the supercurrent. The dipole field $4\pi M$ ($\cong$ a few kG) coming from this is quite negligible compared with the internal molecular field ($\cong$ hundreds kG) arising from the sf interaction in spite that the exchange integral constant is small. To maintain the magnetic induction $B=0$ in a superconductor below T_M a supercurrent must flow on a surface. This effect certainly affects the relative stability of the sn phase, especially the determination of the lower critical transition temperature T_{c2}, but hardly affects the essential feature of the present theory.

It is well known[29,30] that the spatially modulated superconducting state with pairs that break the time-reversal symmetry is depressed by nonmagnetic impurities. Since $ErRh_4B_4$ is thought to be a type-II superconductor with a large Ginzburg-Landau parameter,[31] the coherence length might be comparable to the wavelength of the moment modulation. Therefore we expect that $ErRh_4B_4$ is a relatively clean system and the sn state is not completely destroyed.

As mentioned before the characteristic wave vector $\vec{q}$

of the modulation is determined to satisfy a nesting condition for the spin-up and -down spin split bands. Therefore, the magnitude ($|\vec{q}|=0.06$ Å^{-1}) and direction of the wave vector in ERB must be accounted for by a band-structure calculation.

In conclusion, we propose two crucial experiments on $ErRh_4B_4$ to directly observe the sn phase. One of the most distinctive features of the sn phase that is different from those of the ordinary BCS state is the two-energy-gap structure as shown in Fig. 2, which is rather universal for the incommensurate phase. A far-infrared optical-absorption measurement or a single-particle tunneling experiment might be useful to detect the two-energy-gap structure. Very recently, Lin *et al.*[32] reported interesting single-particle tunneling data on $ErRh_4B_4$, indicating a rich structure in the electron density of states near the Fermi level at around T_M. The structure of five distinctive peaks in the derivative of the conductance in their data and its temperature dependence seem to be in accord with the two energy gaps associated with the sn phase (see Fig. 2).

The neutron experiment near $T_M=1.2$ K is also important. The fundamental wave number rapidly changes continuously from 0 in this narrow temperature region and there is a possibility of observing higher-order satellites.

ACKNOWLEDGMENTS

The authors thank T. Ohmi, S. K. Sinha, S. Takada, T. Koyama, M. Tachiki, H. Yamamoto, A. M. Goldman, L.-J. Lin, and M. Fujita for stimulating discussions. One of the authors (K.M.) thanks G. W. Crabtree, F. Behroozi, D. G. Hinks, L. Hall, I. K. Schuller, and K. E. Grey for useful discussions and their hospitality while he was at Argonne National Laboratory.

APPENDIX

We present a formulation of the helical solution in this appendix. Starting with the BdG equations and the self-consistent equation,

$$\begin{aligned}&(v_Fp+h)u(x)+\Delta(x)v(x)=\epsilon u(x)\ ,\\&(-v_Fp+h)v(x)+\Delta^*(x)u(x)=\epsilon v(x)\ ,\end{aligned}\tag{A1}$$

$$\begin{aligned}&(-v_Fp+h)u'(x)+\Delta(x)v'(x)=\epsilon' u'(x)\ ,\\&(v_Fp+h)v'(x)+\Delta^*(x)u'(x)=\epsilon' v'(x)\ ,\end{aligned}\tag{A2}$$

and

$$\Delta(x)=-g\sum_\nu[v_\nu^*(x)u_\nu(x)f(\epsilon_\nu)+v_\nu'^*(x)u_\nu'(x)f(\epsilon_\nu)]\ ,\tag{A3}$$

we consider the helical solution of the type $\Delta(x)=\tilde{\Delta}e^{2iqx}$. Making the transformations $u(x)=\tilde{u}(x)e^{iqx}$, $v(x)=\tilde{v}(x)e^{-iqx}$, $u'(x)=\tilde{u}'(x)e^{iqx}$, and $v'(x)=\tilde{v}'(x)e^{-iqx}$ we obtain from (A1)

$$\begin{aligned}&(v_Fp+\tilde{q}+h)\tilde{u}(x)+\tilde{\Delta}\tilde{v}(x)=\epsilon\tilde{u}(x)\ ,\\&(-v_Fp+\tilde{q}+h)\tilde{v}(x)+\tilde{\Delta}^*\tilde{u}(x)=\epsilon\tilde{v}(x)\ ,\end{aligned}\tag{A4a}$$

$$\begin{aligned}&(-v_Fp-\tilde{q}+h)\tilde{u}'(x)+\tilde{\Delta}\tilde{v}'(x)=\epsilon'\tilde{u}(x)\ ,\\&(v_Fp-\tilde{q}+h)\tilde{v}'(x)+\tilde{\Delta}^*\tilde{u}'(x)=\epsilon'\tilde{v}'(x)\ ,\end{aligned}\tag{A4b}$$

where $\tilde{q}=v_F\hbar q$. Equation (A4a) immediately leads to the eigenvalue $\epsilon_k=\tilde{q}+h\pm E_k$ with $E_k=[(v_Fk)^2+|\tilde{\Delta}|^2]^{1/2}$. The other BdG equation (A4b) gives the eigenvalue $\epsilon_k'=-\tilde{q}+h\pm E_k$. Thus the resulting free energy $\Omega_{\rm he}$ is expressed as

$$\begin{aligned}\Omega_{\rm he}=&-\frac{1}{\beta L}\sum_k\ln\frac{(1+e^{-\beta(\tilde{q}+h+E_k)})(1+e^{-\beta(\tilde{q}+h-E_k)})}{(1+e^{-\beta(\tilde{q}+h+v_F|k|)})(1+e^{-\beta(\tilde{q}+h-v_F|k|)})}\\&-\frac{1}{\beta L}\sum_k\ln\frac{(1+e^{-\beta(-\tilde{q}+h+E_k)})(1+e^{-\beta(-\tilde{q}+h-E_k)})}{(1+e^{-\beta(-\tilde{q}+h+v_F|k|)})(1+e^{-\beta(-\tilde{q}+h-v_F|k|)})}+\frac{1}{g}|\tilde{\Delta}|^2\ .\end{aligned}\tag{A5}$$

By changing the sum over k into an integral we obtain

$$\begin{aligned}\Omega_{\rm he}=&-\frac{1}{\pi\hbar v_F}\left[|\tilde{\Delta}|^2\left[\ln\frac{\delta_0}{|\tilde{\Delta}|}+\frac{1}{2}\right]\right.\\&+\int_{|\tilde{\Delta}|}^\infty dE(E^2-|\tilde{\Delta}|^2)^{1/2}[f(\tilde{q}+h+E)+f(-\tilde{q}-h+E)+f(-\tilde{q}+h+E)+f(\tilde{q}-h+E)]\\&\left.-\int_0^\infty dE\,E[f(\tilde{q}+h+E)+f(-\tilde{q}-h+E)+f(-\tilde{q}+h+E)+f(\tilde{q}-h+E)]\right]\ .\end{aligned}\tag{A6}$$

The minimization of $\Omega_{\rm he}$ with respect to $|\tilde{\Delta}|$ yields the gap equation,

$$2\ln\frac{\delta_0}{|\tilde{\Delta}|}-\int_{|\tilde{\Delta}|}^\infty dE\frac{1}{(E^2-|\tilde{\Delta}|^2)^{1/2}}[f(\tilde{q}+h+E)+f(-\tilde{q}-h+E)+f(-\tilde{q}+h+E)+f(\tilde{q}-h+E)]=0\ .\tag{A7}$$

In order to determine the wave number q we differentiate $\Omega_{\rm he}$ with respect to q, that is, we obtain

$$\int_{|\tilde{\Delta}|}^{\infty} dE(E^2-|\tilde{\Delta}|^2)^{1/2}[f'(\tilde{q}+h+E)-f'(-\tilde{q}-h+E)-f'(-\tilde{q}+h+E)+f'(\tilde{q}-h+E)] - \int_0^{\infty} dE\,E[f'(\tilde{q}+h+E)-f'(-\tilde{q}-h+E)-f'(-\tilde{q}+h+E)+f'(\tilde{q}-h+E)]=0 . \quad \text{(A8)}$$

The coupled equations [(A7) and (A8)] completely determine $|\tilde{\Delta}|$ and q. By allowing $|\tilde{\Delta}|\to 0$ and $T\to T_c$, we obtain from Eq. (A7)

$$\ln\frac{2\tilde{q}_s}{\delta_0}-\int_0^{\tilde{q}_s} d\xi\frac{1}{\xi}[f(\tilde{q}+h+\xi)-f(\tilde{q}+h-\xi)+f(-\tilde{q}+h+\xi)-f(-\tilde{q}+h-\xi)]=0 . \quad \text{(A9)}$$

This coincides with Eq. (4.5) if we identify $\tilde{q}$ with δ. This means that the boundary between the normal and the helical phase coincides with that between the normal and the sn phase. This fact was already pointed out by Larkin and Ovchinnikov.[14]

The numerical computation of $\Omega_{\rm he}$ in Eq. (A5) reveals that (1) the critical field $h_{\rm cr}$ beyond which the helical phase is stabilized over the BCS phase is given by $h_{\rm cr}=0.68\delta_0$, and (2) the transition from the BCS to the helical phase is of first order. This agrees with the previous calculation by using the three-dimensional model.[13–15]

[1]See, for example, M. Ishikawa, Cont. Phys. **23**, 443 (1983); *Superconductivity in Ternary Compounds,* edited by M. B. Maple and Ø. Fischer (Springer, New York, 1982), Vols. 1 and 2.

[2]S. K. Sinha, G. W. Crabtree, D. G. Hinks, and H. Mook, Phys. Rev. Lett. **48**, 950 (1982), and also see S. K. Sinha, G. W. Crabtree, D. G. Hinks, H. A. Mook, and O. A. Pringle, J. Magn. Magn. Mater. **31-34**, 489 (1983).

[3]D. E. Moncton, D. B. McWhan, P. H. Schmidt, G. Shirane, W. Thomlinson, M. B. Maple, H. B. MacKay, L. D. Woolf, Z. Fisk, and D. C. Johnston, Phys. Rev. Lett. **45**, 2060 (1980).

[4]J. W. Lynn, D. E. Moncton, W. Thomlinson, G. Shirane, and R. N. Shelton, Solid State Commun. **26**, 493 (1978); J. W. Lynn, G. Shirane, W. Thomlinson, and R. N. Shelton, Phys. Rev. Lett. **46**, 368 (1981).

[5]H. Matsumoto, H. Umezawa, and M. Tachiki, Solid State Commun. **31**, 157 (1979); M. Tachiki, A. Kotani, H. Matsumoto, and H. Umezawa, *ibid.* **31**, 927 (1979).

[6]E. I. Blount and C. M. Varma, Phys. Rev. Lett. **42**, 1079 (1979); H. S. Greenside, E. I. Blount, and C. M. Varma, *ibid.* **46**, 49 (1981).

[7]R. A. Ferrell, J. K. Bhattacharjee, and A. Bagchi, Phys. Rev. Lett. **43**, 154 (1979).

[8]M. Tachiki, H. Matsumoto, T. Koyama, and H. Umezawa, Solid State Commun. **34**, 19 (1980).

[9]C. G. Kuper, M. Revzen, and A. Ron, Phys. Rev. Lett. **44**, 1545 (1980).

[10]K. Machida, J. Phys. Soc. Jpn. **51**, 3462 (1982).

[11]K. Machida, J. Phys. Soc. Jpn. **52**, 2181 (1983).

[12]K. Machida, K. Nokura, and T. Matsubara, Phys. Rev. B **22**, 2307 (1980).

[13]P. Fulde and R. A. Ferrell, Phys. Rev. **135**, A550 (1964).

[14]A. I. Larkin and Y. N. Ovchinnikov, Zh. Eksp. Teor. Fiz. **47**, 1136 (1964) [Sov. Phys.—JETP **20**, 762 (1965)].

[15]S. Takada and T. Izuyama, Prog. Theor. Phys. **41**, 635 (1969).

[16]T. M. Rice, Phys. Rev. B **2**, 3619 (1970).

[17]S. A. Brazovskii, S. A. Gordynin, and N. N. Kirova, Pis'ma Zh. Eksp. Teor. Fiz. **31**, 486 (1980) [JETP Lett. **31**, 456 (1980)].

[18]J. Mertsching and H. J. Fischbeck, Phys. Status Solidi B **103**, 783 (1981).

[19]B. Horovitz, Phys. Rev. Lett. **46**, 742 (1981).

[20]P. G. de Gennes, *Superconductivity of Metals and Alloys* (Benjamin, New York, 1966).

[21]H. Takayama, Y. R. Lin-Liu, and K. Maki, Phys. Rev. B **21**, 2388 (1980). Also see H. Yamamoto and T. Ohmi, Prog. Theor. Phys. **66**, 805 (1981).

[22]E. T. Whittaker and G. N. Watson, *A Course of Modern Analysis,* 4th ed. (Cambridge University Press, Cambridge, England, 1927).

[23]K. Maki and T. Tsuneto, Prog. Theor. Phys. **31**, 945 (1964).

[24]M. C. Leung, Phys. Rev. B **11**, 4272 (1975).

[25]K. Machida and D. Youngner, J. Low Temp. Phys. **35**, 449 (1979); **35**, 561 (1979); D. Youngner and K. Machida, *ibid.* **36**, 617 (1979).

[26]G. W. Crabtree, F. Behroozi, S. A. Campbell, and D. G. Hinks, Phys. Rev. Lett. **49**, 1342 (1982); F. Behroozi, G. W. Crabtree, S. A. Campbell, and D. G. Hinks, Phys. Rev. B **27**, 6849 (1983).

[27]K. Machida, J. Low Temp. Phys. **53**, 403 (1983).

[28]S. K. Sinha and J. K. Kjems (private communication).

[29]S. Takada, Prog. Theor. Phys. **43**, 27 (1970).

[30]L. G. Aslamazov, Zh. Eksp. Teor. Fiz. **55**, 1477 (1968) [Sov. Phys.—JETP **28**, 773 (1969)].

[31]L. D. Woolf, D. C. Johnston, H. B. MacKay, R. W. McCallum, and M. P. Maple, J. Low. Temp. Phys. **35**, 651 (1979).

[32]L.-J. Lin, A. M. Goldman, A. M. Kadin, and C. P. Umbach, Phys. Rev. Lett. **51**, 2151 (1983).